

Workshop on “Towards a consistent approach for nuclear structure and reactions: microscopic optical potentials”

ECT*, 17 – 21, June 2024

Extracting neutron skin from elastic proton-nucleus scattering with deep neural network

Guohao Yang (杨国浩)

School of Physical Science and Technology, Southwest University, China

G. H. Yang, Y. Kuang, Z. X. Yang[†], and Z. P. Li[‡], arXiv:2311.11676

[†] zuxing.yang@riken.jp

[‡] zpliphy@swu.edu.cn

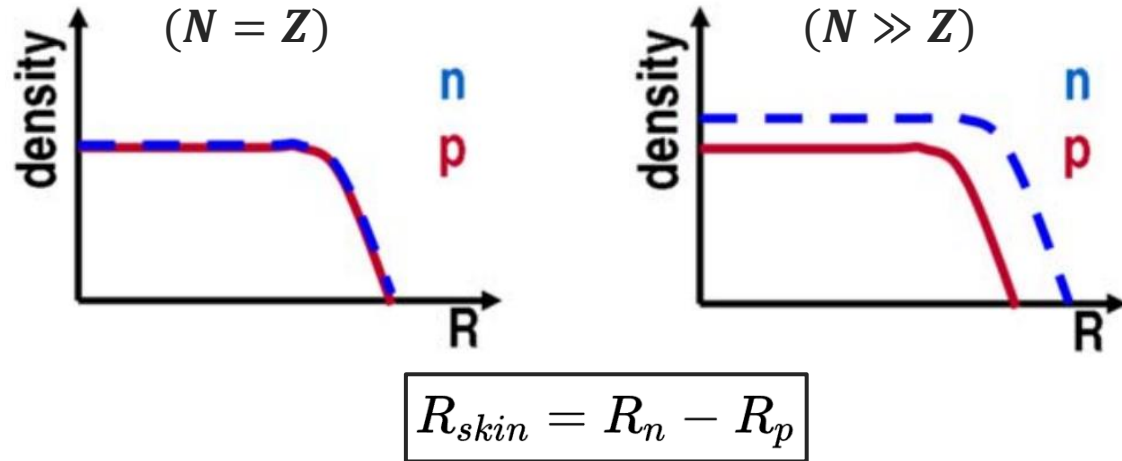


Contents



- Introduction
- Theoretical framework
 - ✓ Relativistic Impulse Approximation (RIA) theory
 - ✓ Back-propagation neural network
- Results and discussion
- Summary

Study on neutron skin thickness



Measurement:

- R_n : parity-violating
- R_p : elastic electron scattering

C. J. Horowitz, *et al.*, JPG 41, 093001 (2014).

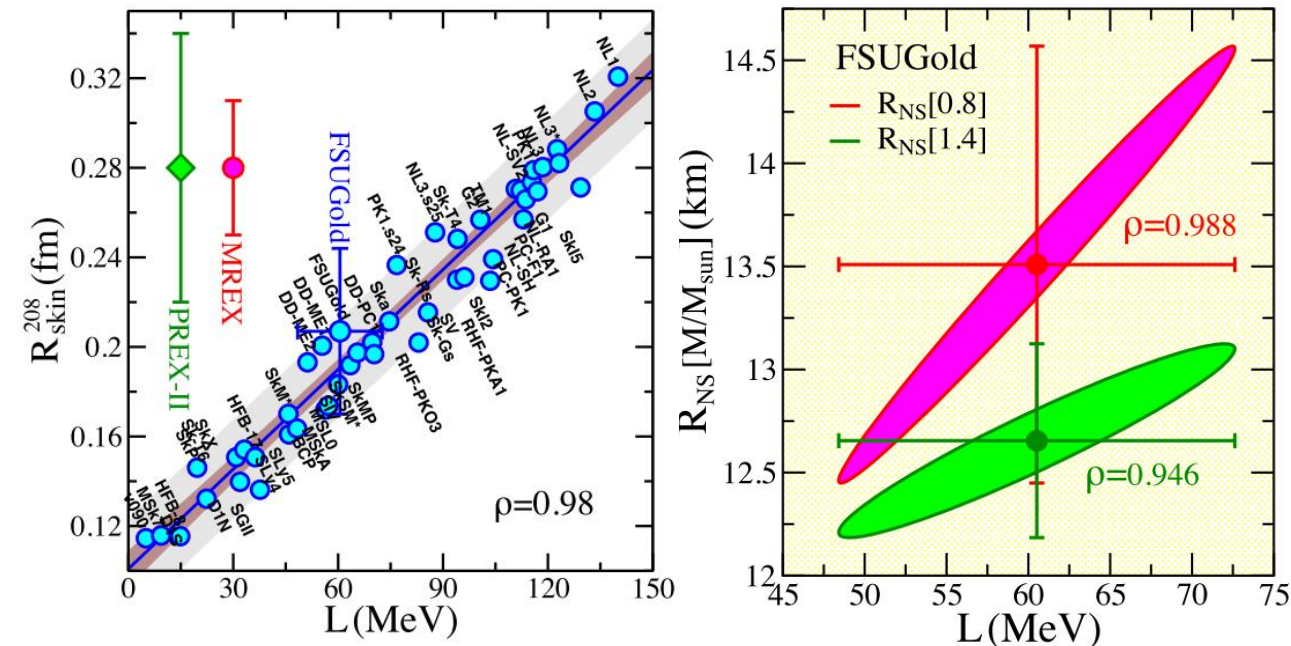
Moreover :

- coherent pion-photo production
- measurements of electric dipole polarizabilities

C. M. Tarbert, *et al.* PRL. 112, 242502 (2014).

A. Tamii, *et al.*, PRL. 107, 062502 (2011).

.....



M. Thiel, *et al.*, JPG 46, 093003 (2019).

□ Based on **elastic proton-nucleus scattering experiments**:

● Glauber multiple scattering theory

Li, Kuang, Huang, Tu, Li, *et al.*, PRC 107, 064310 (2023).

Zhang, Ma, Huang, Tu, *et al.*, PRC 108, 014614 (2023)

.....

● Brueckner theory + g-matrix folding model

S. Karataglidis, *et al.*, PRC 65, 044306 (2002).

S. Tagami, *et al.*, Results in Physics 33, 105155 (2022).

.....

● Relativistic Impulse Approximation (RIA) theory + two-parameter Fermi (2pF) model

B. C. Clark, S. Hama, *et al.*, PRL. 50, 1644 (1983).

D. P. Murdock and C. J. Horowitz, PRC 35, 1442 (1987)

Terashima, Sakaguchi, Takeda, *et al.*, PRC 77, 024317 (2008).

Zenihiro, Sakaguchi, Murakami, *et al.*, PRC 82, 044611 (2010).

Matsuda, Sakaguchi, Takeda, *et al.*, PRC 87, 034614 (2013).

Zenihiro, Sakaguchi, Terashima, *et al.*, arXiv (2018)

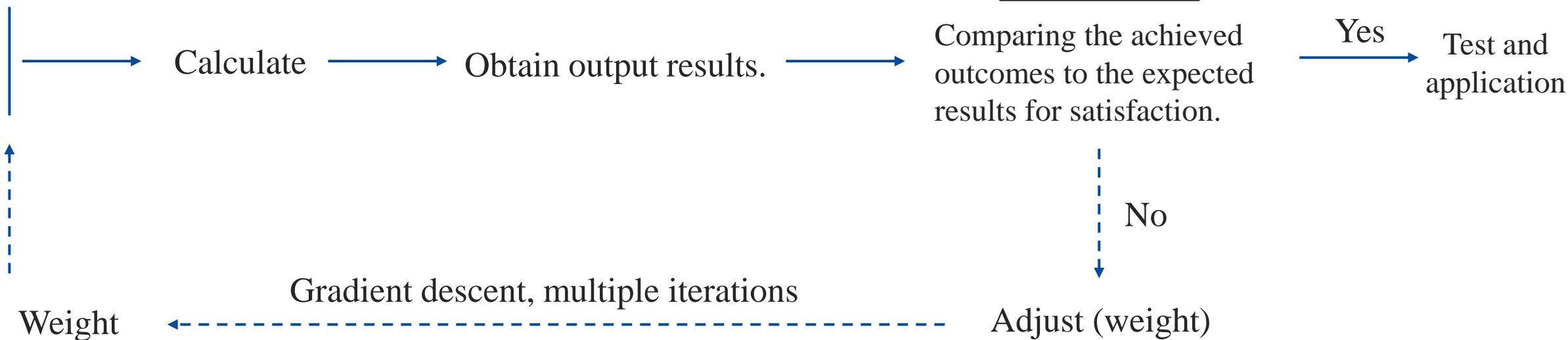
.....

Two-parameter Fermi model is too simple.

- **Deep neural network is a very effective method to represent complex function.**

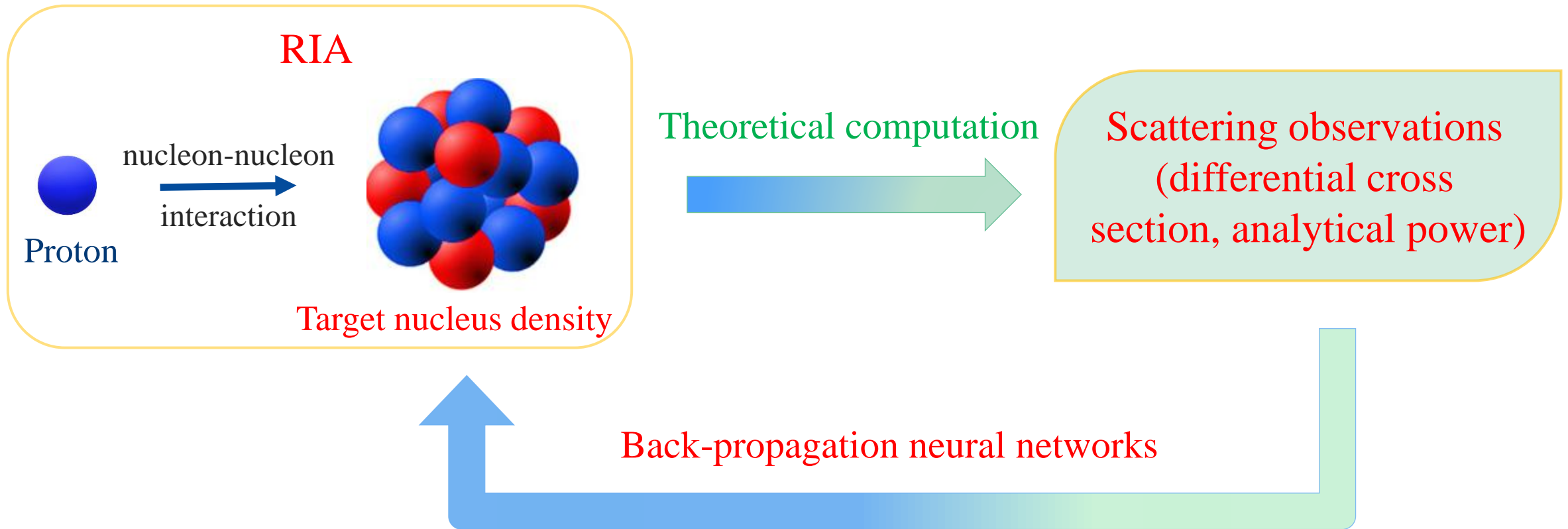
Nuclear charge radius, Nuclear mass, Nuclear half-life, fission yields.....

Training samples



Combining deep neural network with RIA theory could help overcome limitations in previous studies.

To combine RIA and deep neural network to infer the density distribution and extract neutron skin thickness.





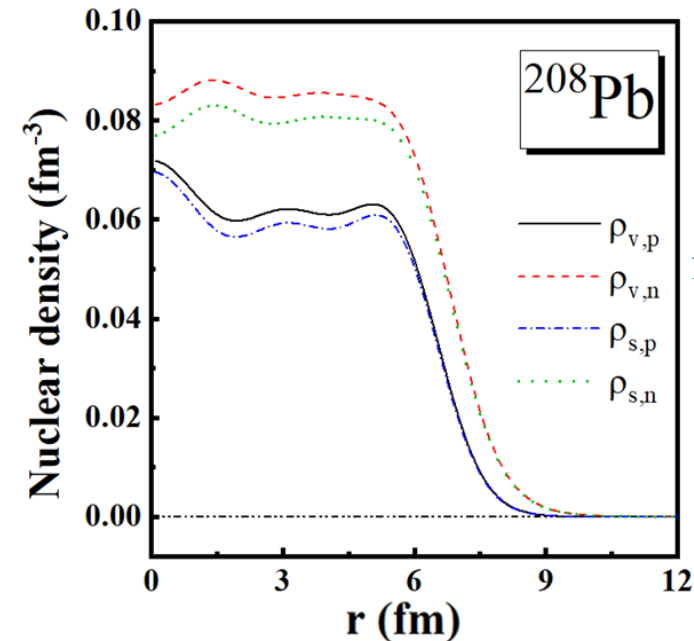
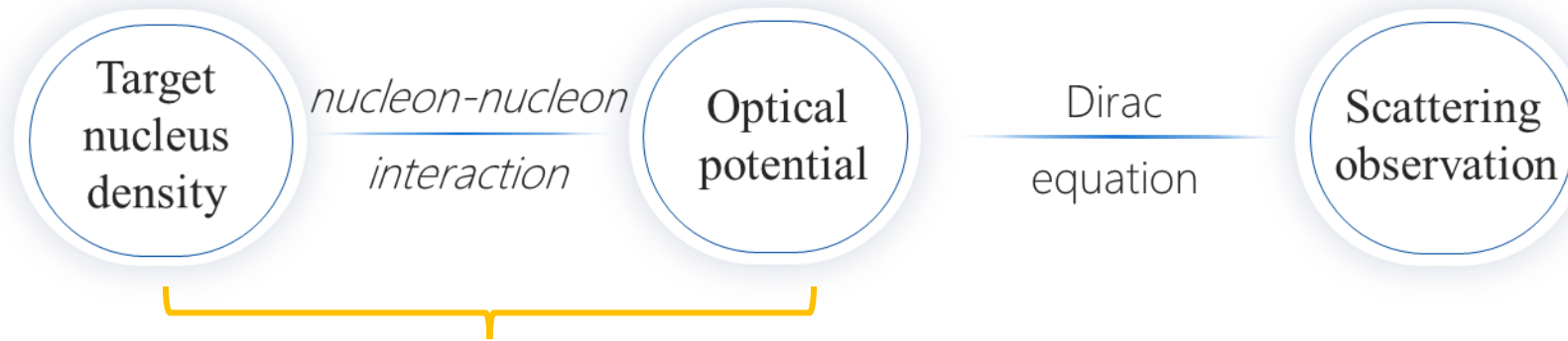
Contents



- Introduction
- Theoretical framework
 - ✓ Relativistic Impulse Approximation (RIA) theory
 - ✓ Back-propagation neural network
- Results and discussion
- Summary

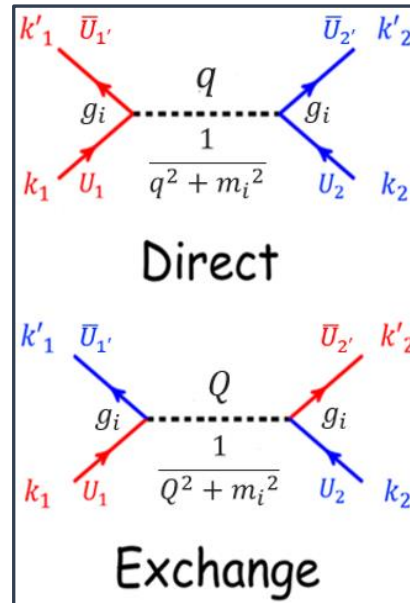
Relativistic Impulse Approximation (RIA) theory

□ The RIA forward process



Target nucleus density

folding



nucleon-nucleon interaction

$$U_{\text{opt}}(r, E) = \sum_L [U_D^L(r, E) + U_X^L(r, E)] \lambda^L$$

- Direct term

$$U_D^L(r, E) = -\frac{4\pi ip}{M} \int d^3r' \rho_L(\mathbf{r}') t_D^L(|\mathbf{r}' - \mathbf{r}|; E)$$

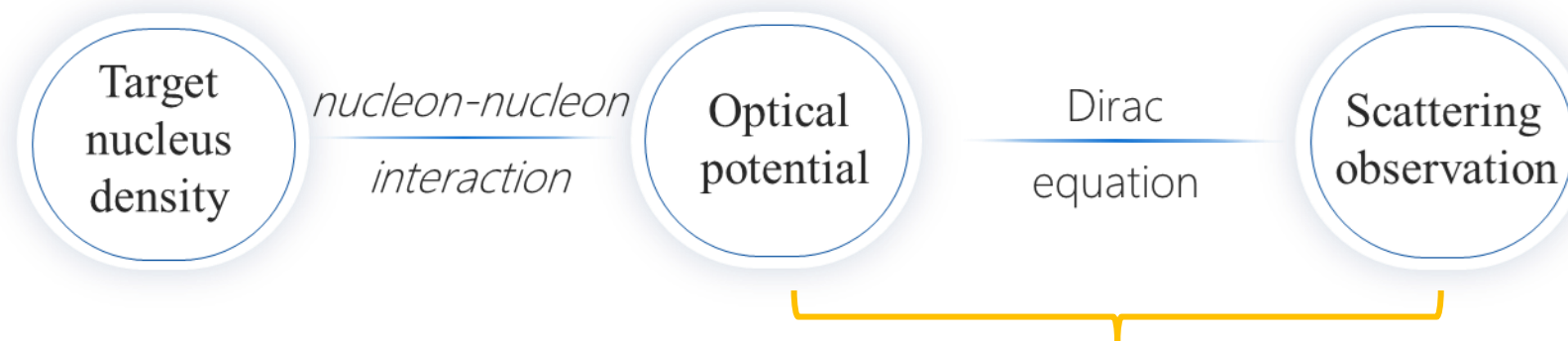
- Exchange term

$$U_X^L(r, E) = -\frac{4\pi ip}{M} \int d^3r' \rho_L(\mathbf{r}', \mathbf{r}) t_X^L(|\mathbf{r}' - \mathbf{r}|; E) j_0(p|\mathbf{r}' - \mathbf{r}|)$$

Optical potential

Relativistic Impulse Approximation (RIA) theory

□ The RIA forward process



$$hU_0(\mathbf{r}) = \left\{ -i\boldsymbol{\alpha} \cdot \nabla + \underbrace{U^V}_{\text{Vector potential}}(\mathbf{r}; E) + \beta \left[M + \underbrace{U^S}_{\text{Scalar potential}}(\mathbf{r}; E) \right] \right\} U_0(\mathbf{r}) = EU_0(\mathbf{r})$$

Differential cross section

$$\frac{d\sigma}{d\Omega} = |A(\theta)|^2 + |B(\theta)|^2$$

Scattering amplitude

$$A(\theta) = f_c(\theta) + \frac{1}{k} \sum_l e^{2i\sigma_l} [(l+1)\mathcal{C}_{l,l+1/2} + l\mathcal{C}_{l,l-1/2}] P_l(\cos\theta)$$

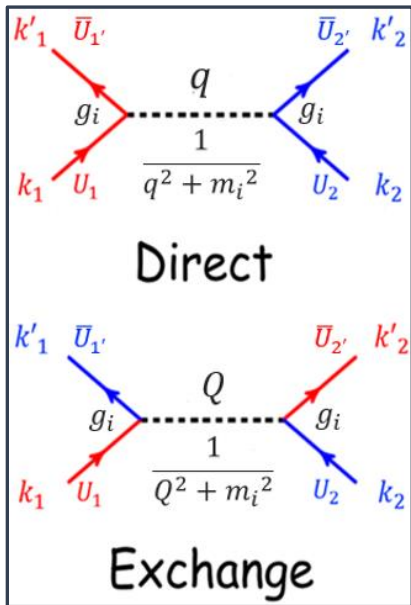
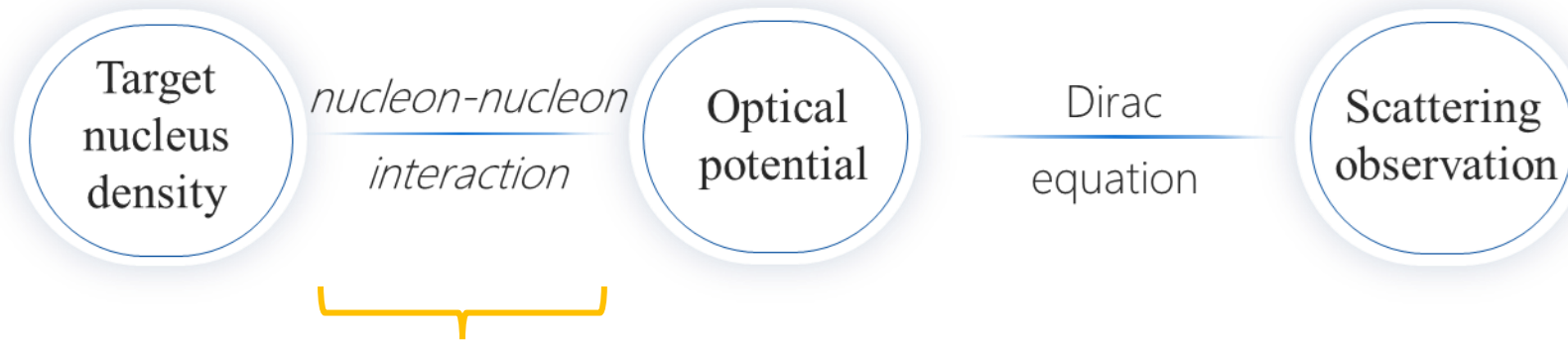
Analysis power

$$A_y = \frac{2\text{Re}[A^*(\theta)B(\theta)]}{d\sigma/d\Omega}$$

$$B(\theta) = \frac{i}{k} \sum_l e^{2i\sigma_l} [\mathcal{C}_{l,l+1/2} - \mathcal{C}_{l,l-1/2}] P_l^1(\cos\theta)$$

Interaction involving the medium effects

□ The RIA forward process



- Direct term

$$F_D^L(q) = \sum_{i=1}^N \delta_{L,L(i)} \langle \vec{\tau}_1 \cdot \vec{\tau}_2 \rangle^{T_i} f^i(q)$$

- Exchange term

$$F_X^L(Q) = (-1)^{T_{NN}} \sum_{i=1}^N C_{L(i),L} \langle \vec{\tau}_1 \cdot \vec{\tau}_2 \rangle^{T_i} f^i(Q)$$

$$f^i(x) = \frac{g_i^2}{x^2 + m_i^2} \left(1 + \frac{x^2}{\Lambda_i^2} \right)^{-2} - i \frac{\bar{g}_i^2}{x^2 + \bar{m}_i^2} \left(1 + \frac{x^2}{\bar{\Lambda}_i^2} \right)^{-2}$$

- Momentum space

$$t_D^L(q, E) \equiv (iM^2 / 2E_c k_c) F_D^L(q)$$

$$t_X^L(q, E) \equiv (iM^2 / 2E_c k_c) F_X^L(q)$$

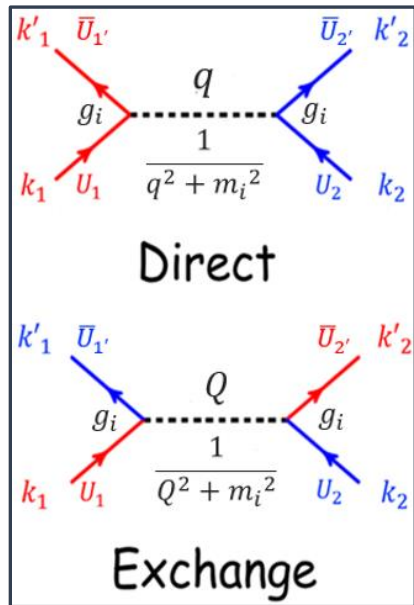
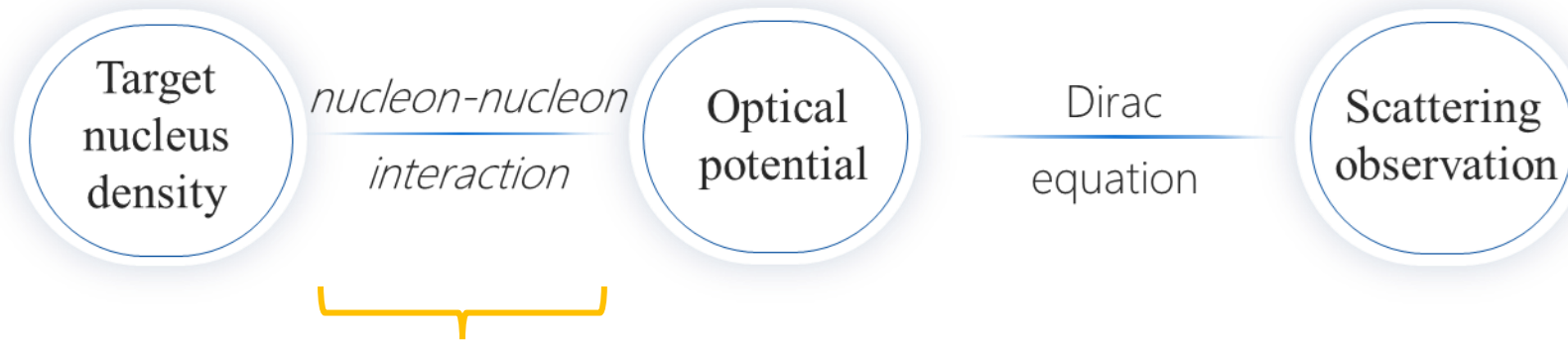
- Coordinate space

$$t_D^L(|\mathbf{r}' - \mathbf{r}|; E) \equiv \int \frac{d^3q}{(2\pi)^3} t_D^L(q, E) e^{-i\mathbf{q}\cdot\mathbf{r}}$$

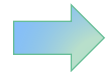
$$t_X^L(|\mathbf{r}' - \mathbf{r}|; E) \equiv \int \frac{d^3q}{(2\pi)^3} t_X^L(q, E) e^{-i\mathbf{q}\cdot\mathbf{r}}$$

Interaction involving the medium effects

□ The RIA forward process



$$f^i(x) = \frac{g_i^2}{x^2 + m_i^2} \left(1 + \frac{x^2}{\Lambda_i^2}\right)^{-2} - i \frac{\bar{g}_i^2}{x^2 + \bar{m}_i^2} \left(1 + \frac{x^2}{\bar{\Lambda}_i^2}\right)^{-2}$$



$$g_i^2 \longrightarrow \frac{g_i^2}{1 + a_i \rho(r) / \rho_0}$$

$$\bar{g}_i^2 \longrightarrow \frac{\bar{g}_i^2}{1 + \bar{a}_i \rho(r) / \rho_0}$$

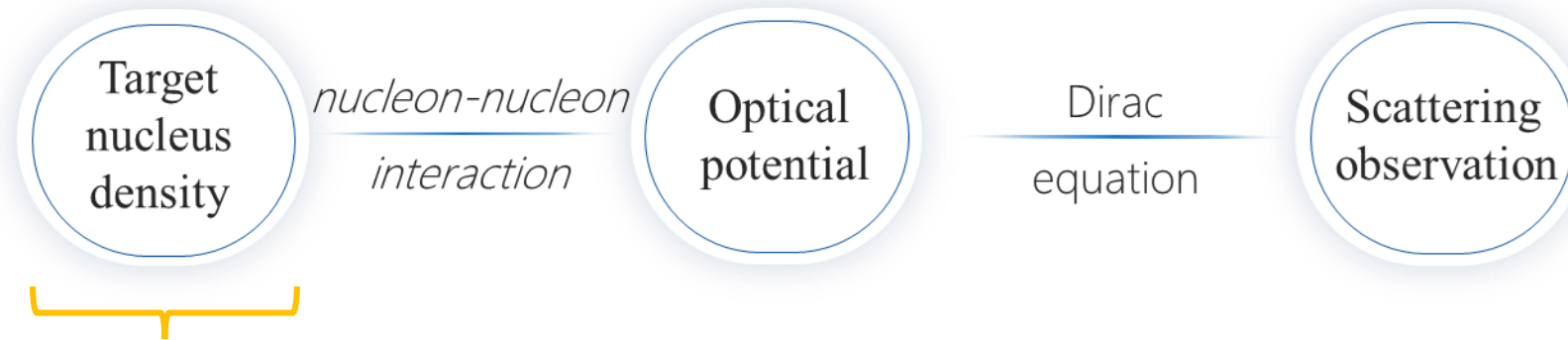
H. Sakaguchi *et al.*, Phys. Rev. C 57, 1749 (1998).

S. Terashima, *et al.*, Phys. Rev. C 77, 024317 (2008).

$$i = (\sigma, \omega) \quad \rho_0 = 0.1934 \text{ fm}^{-3}$$

Interaction involving the medium effects

□ The RIA forward process

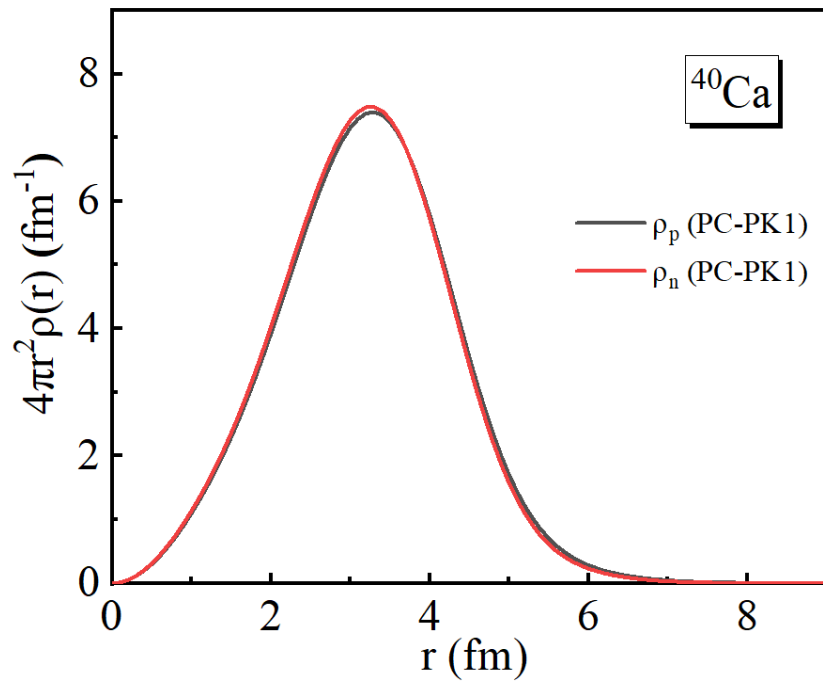
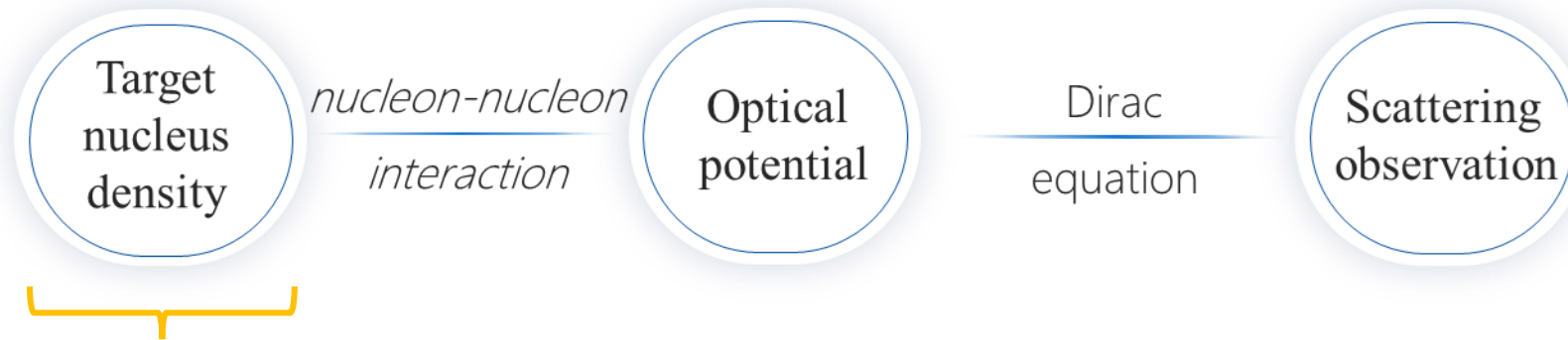


For ^{40}Ca :

Proton vector density ρ_p :	√	(From experiment)
Neutron vector density ρ_n :	×	
Proton scalar density $\rho_{p,s}$:	×	
Neutron scalar density $\rho_{n,s}$:	×	

Interaction involving the medium effects

□ The RIA forward process



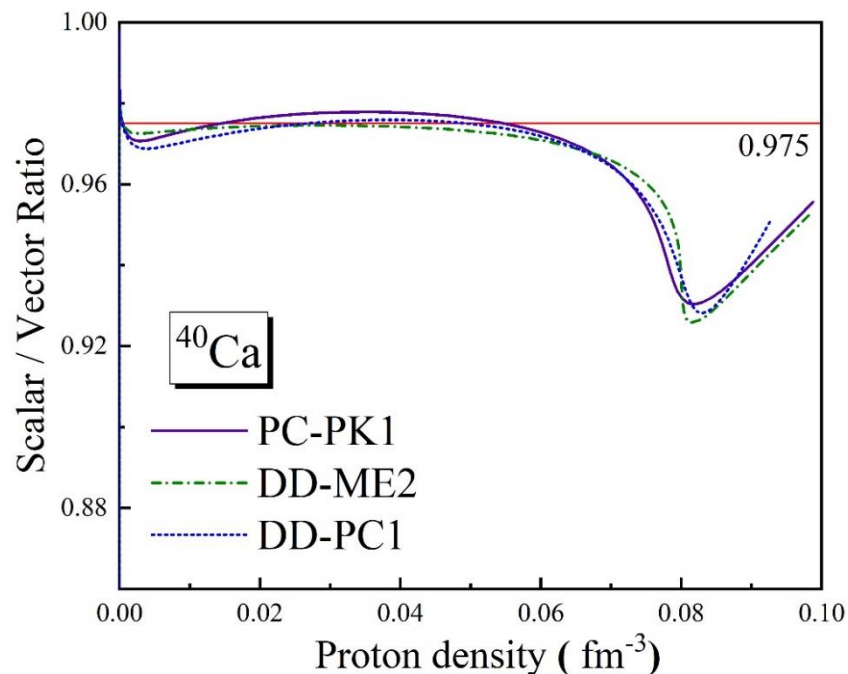
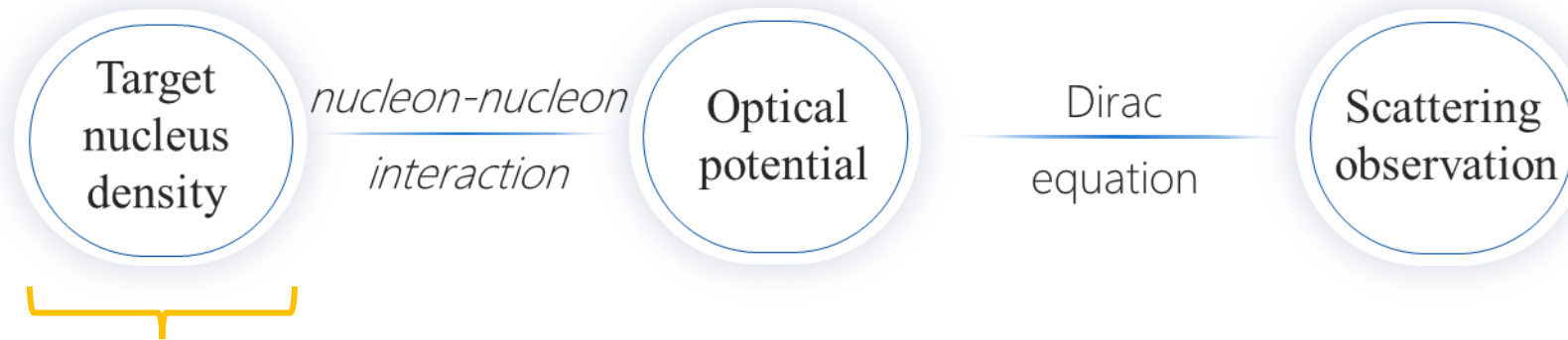
□ Assuming the neutron density distribution

S. Terashima, *et al.*, *Phys. Rev. C* 77, 024317 (2008).

$$\rho_n = \rho_p$$

Interaction involving the medium effects

□ The RIA forward process



□ The ratio of scalar to vector density is 0.975

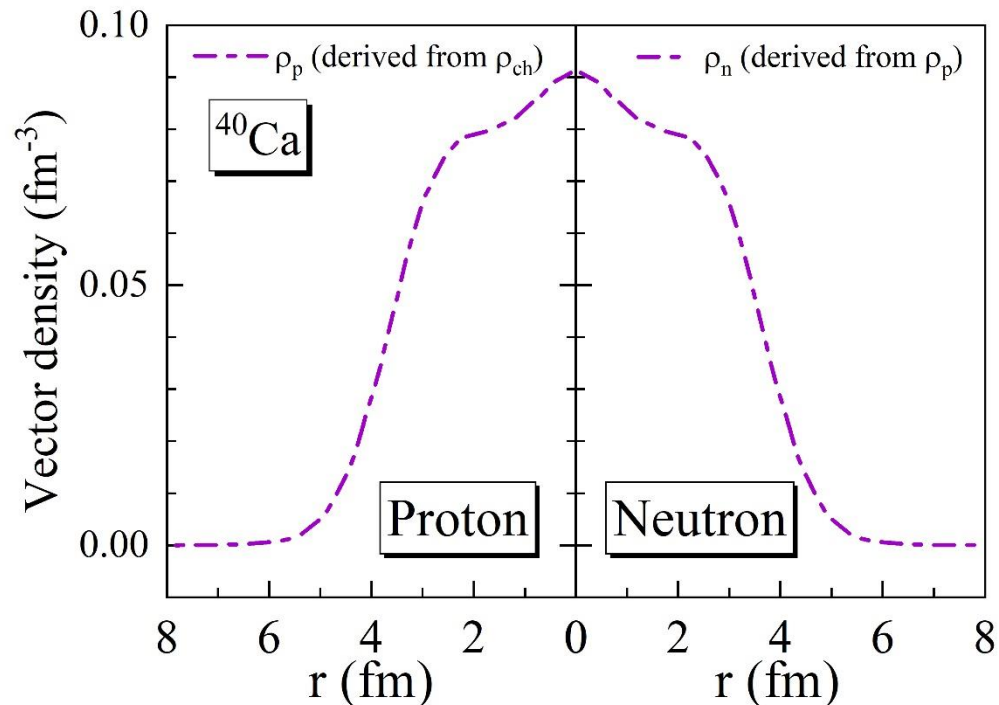
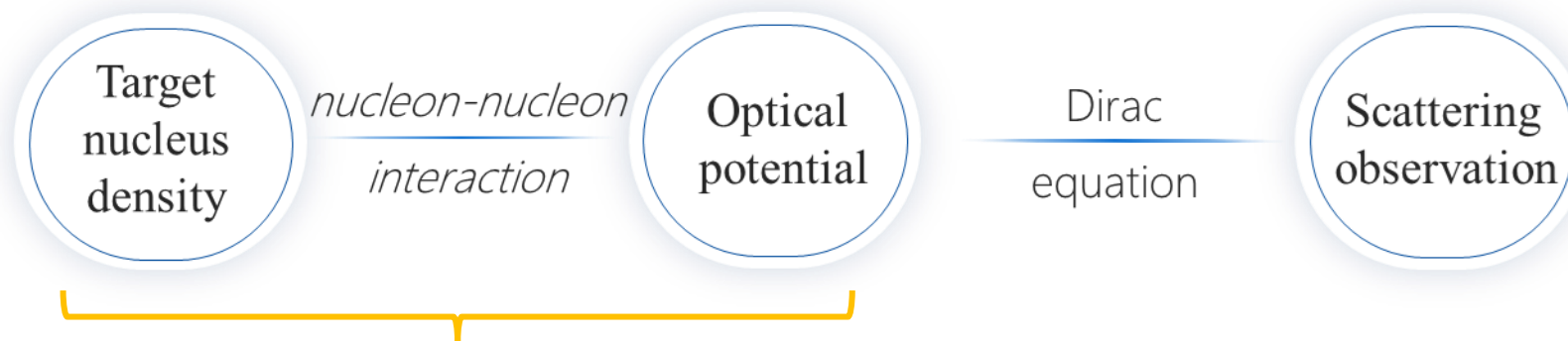
S. Terashima, *et al.*, Phys. Rev. C 77, 024317 (2008).

$$\rho_{p,s} = 0.975 \rho_p$$

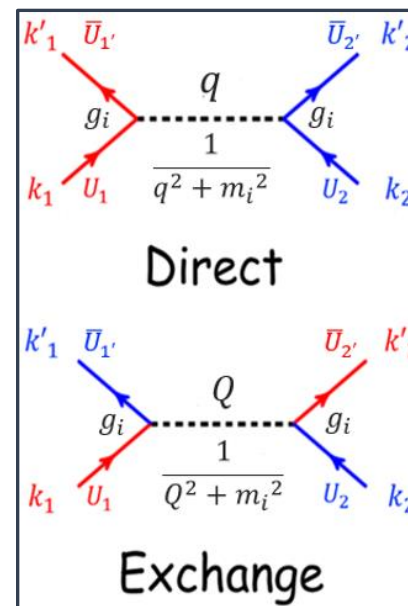
$$\rho_{n,s} = 0.975 \rho_n$$

Interaction involving the medium effects

□ The RIA forward process



folding \longleftrightarrow



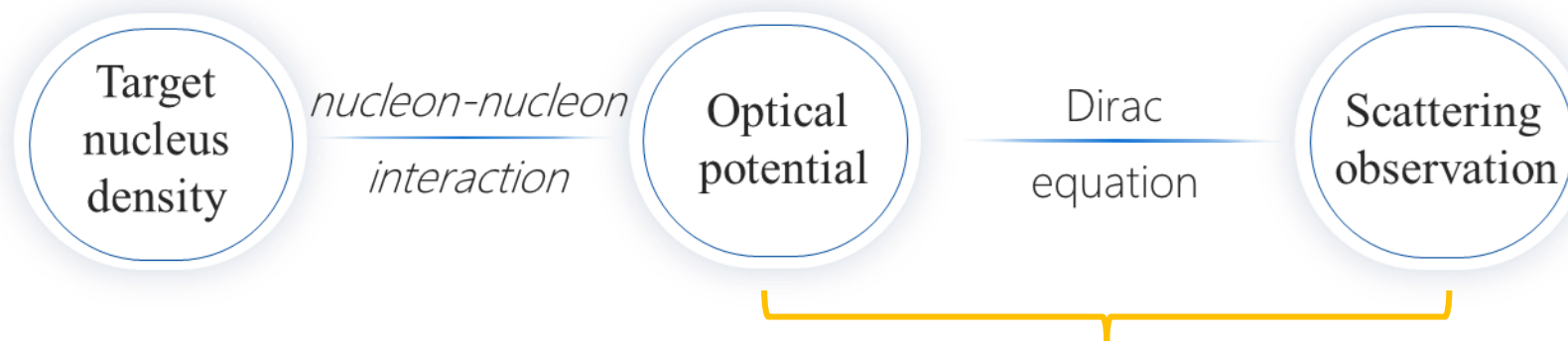
$$g_i^2 \longrightarrow \frac{g_i^2}{1 + a_i \rho(r) / \rho_0}$$

$$\bar{g}_i^2 \longrightarrow \frac{\bar{g}_i^2}{1 + \bar{a}_i \rho(r) / \rho_0}$$

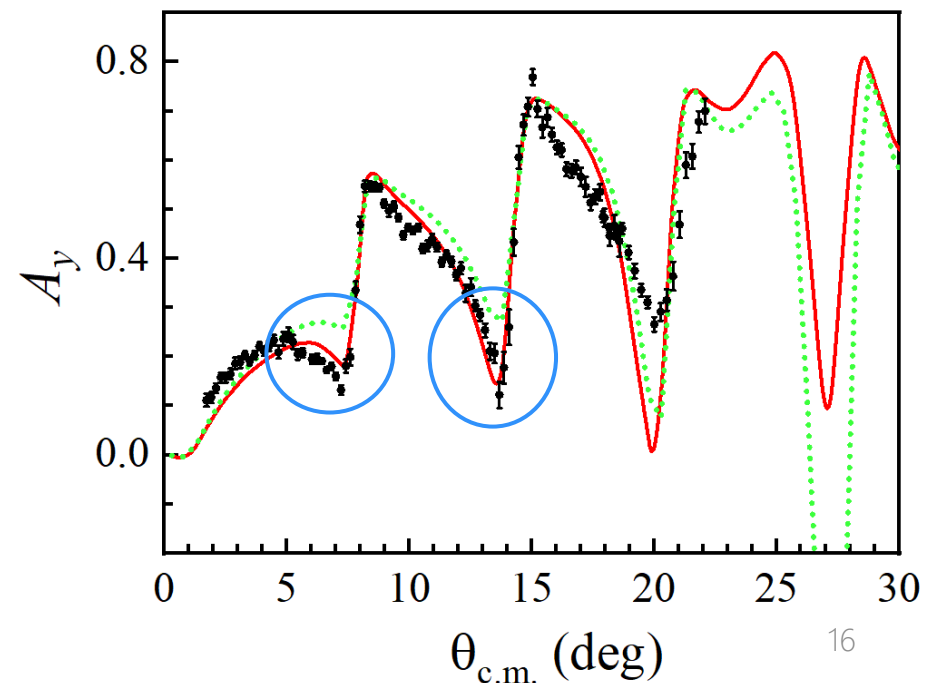
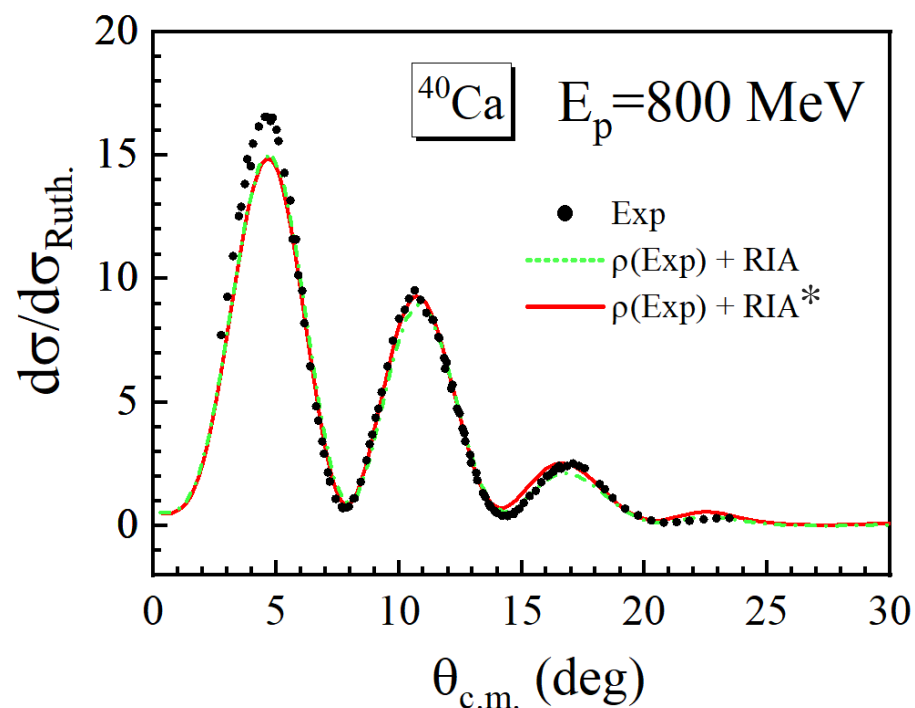
$$i = (\sigma, \omega) \quad \rho_0 = 0.1934 \text{ fm}^{-3}$$

Interaction involving the medium effects

□ The RIA forward process



$$\begin{aligned} a_{\sigma} &= 0.160 \\ \bar{a}_{\sigma} &= -0.649 \\ a_{\omega} &= 0.149 \\ \bar{a}_{\omega} &= -0.310 \end{aligned}$$



Back-propagation neural network

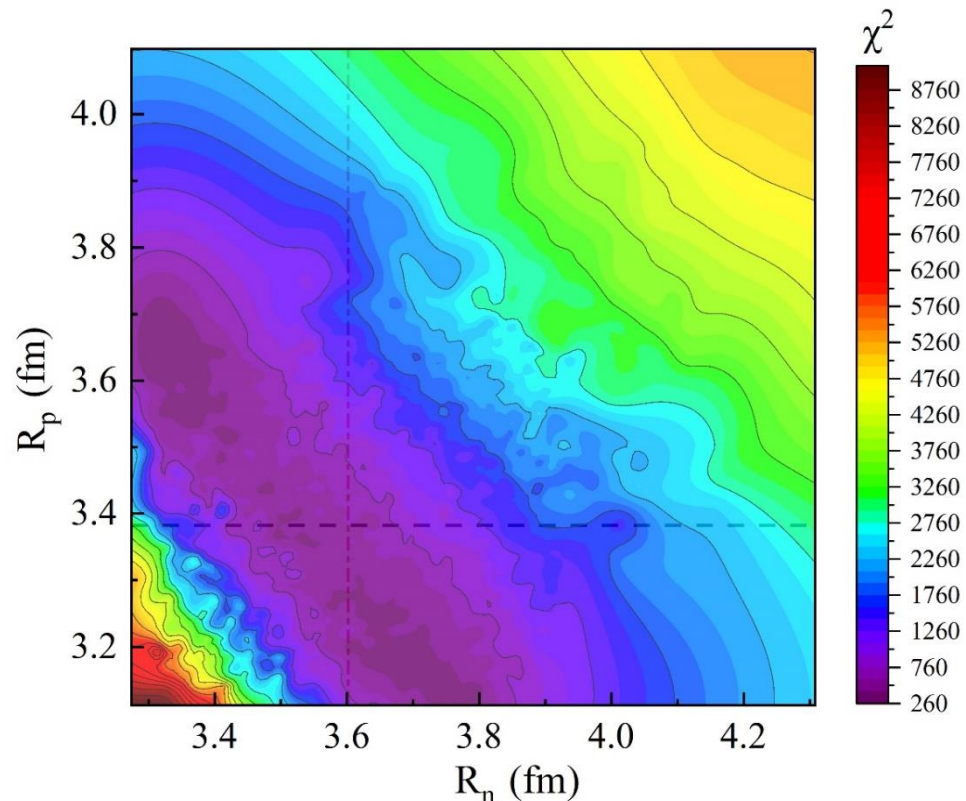
□ Density composition of the ^{48}Ca training dataset

Relativistic Hartree-Bogoliubov : DD-ME2, PC-PK1, DD-PK1

Relativistic mean field : PK1

Skyrme-Hartree-Fock : 24 Sets parameters

□ Contour plot of the training set observations for χ^2 .



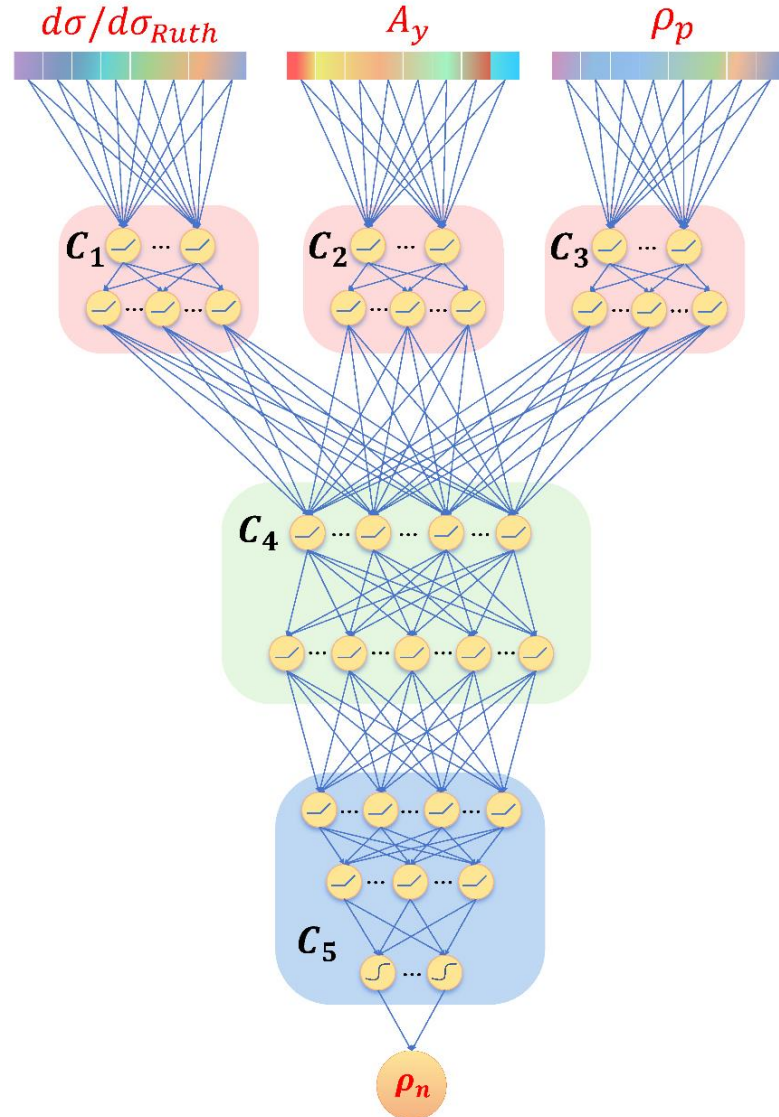
$$\chi^2 = \sum [(x_{\text{exp.}} - x_{\text{theo.}}) / \Delta x_{\text{exp.}}]^2$$


where $x_{\text{exp.}}$, $\Delta x_{\text{exp.}}$, and $x_{\text{theo.}}$ are the experimental data, the errors in the data, and the calculation results, respectively.

□ The training dataset covers a wide range of neutron and proton radii.

Back-propagation neural network

observable-to-density network (OTDN)



ReLU :  Sigmoid : 

- Loss function (Normalized flow of Pearson χ^2 divergence (NPD))

$$\text{NPD} = \left\langle \frac{[\mu \rho_{\text{pre}}(r) - \rho_{\text{tar}}(r)]^2}{\mu \rho_{\text{pre}}(r)} \right\rangle$$

$$\mu = \frac{N}{\int_0^\infty 4\pi \rho_{\text{pre}}(r) r^2 dr}$$

- μ is the normalization factor.

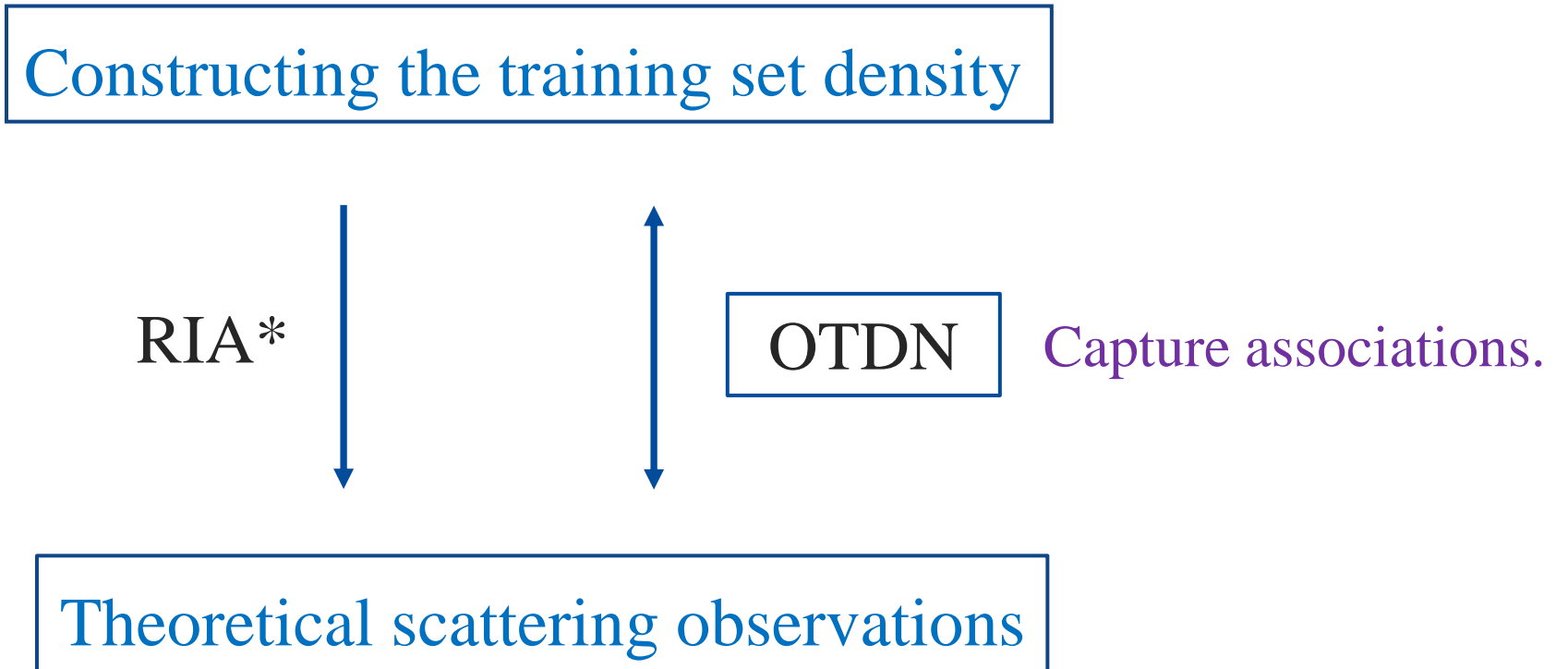


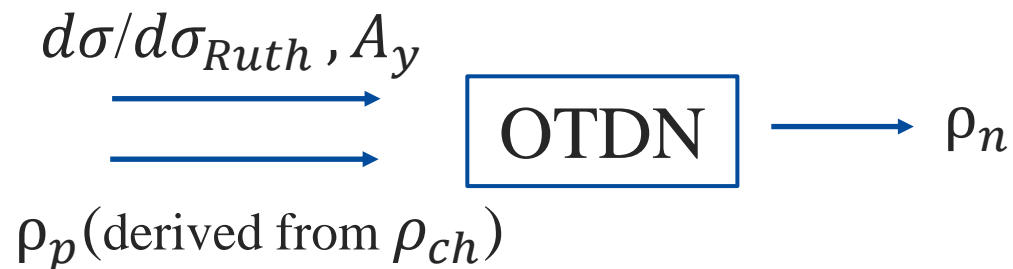
Contents



- Introduction
- Theoretical framework
 - ✓ Relativistic Impulse Approximation (RIA) theory
 - ✓ Back-propagation neural network
- Results and discussion
- Summary

Bayesian model averaging (BMA)



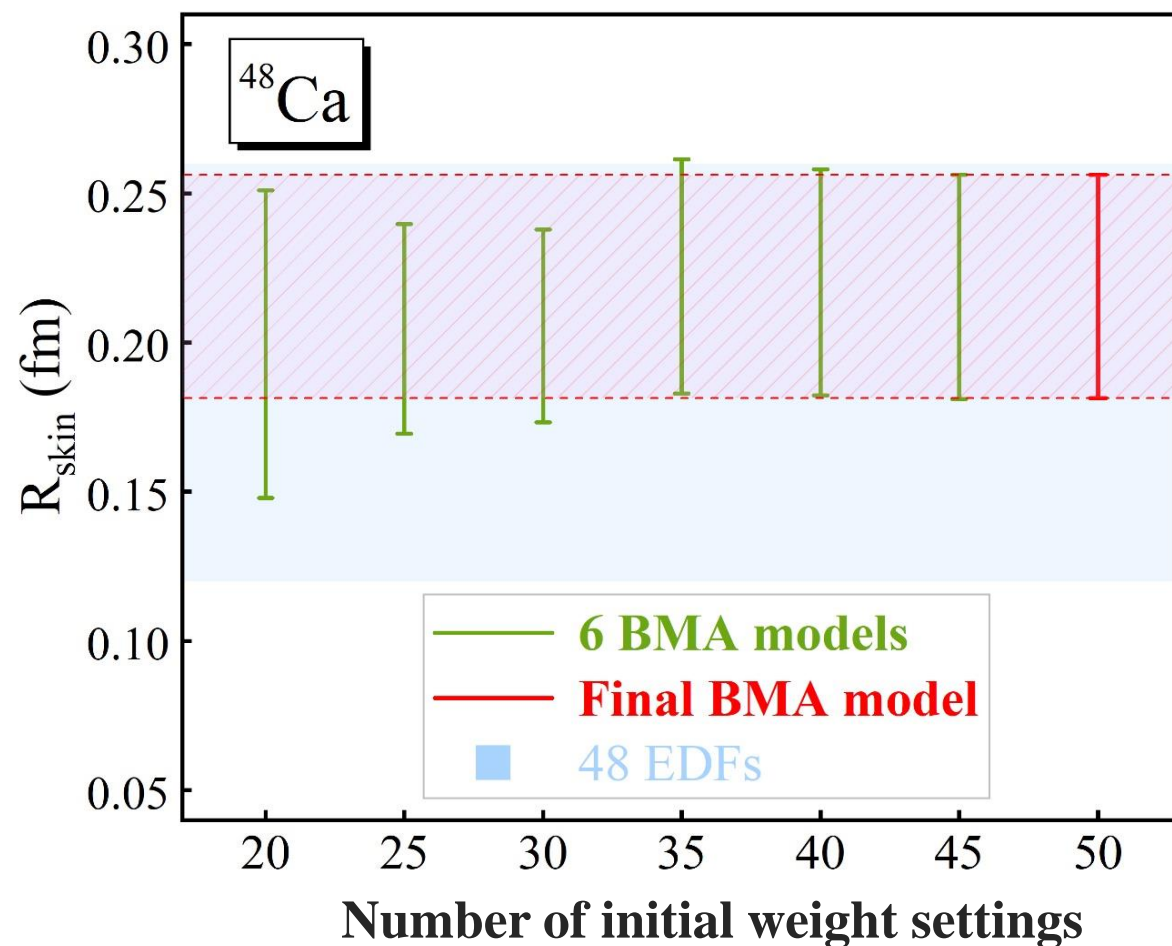


- Different initial weight settings lead to different results.

How to eliminate errors from different initial weight settings?

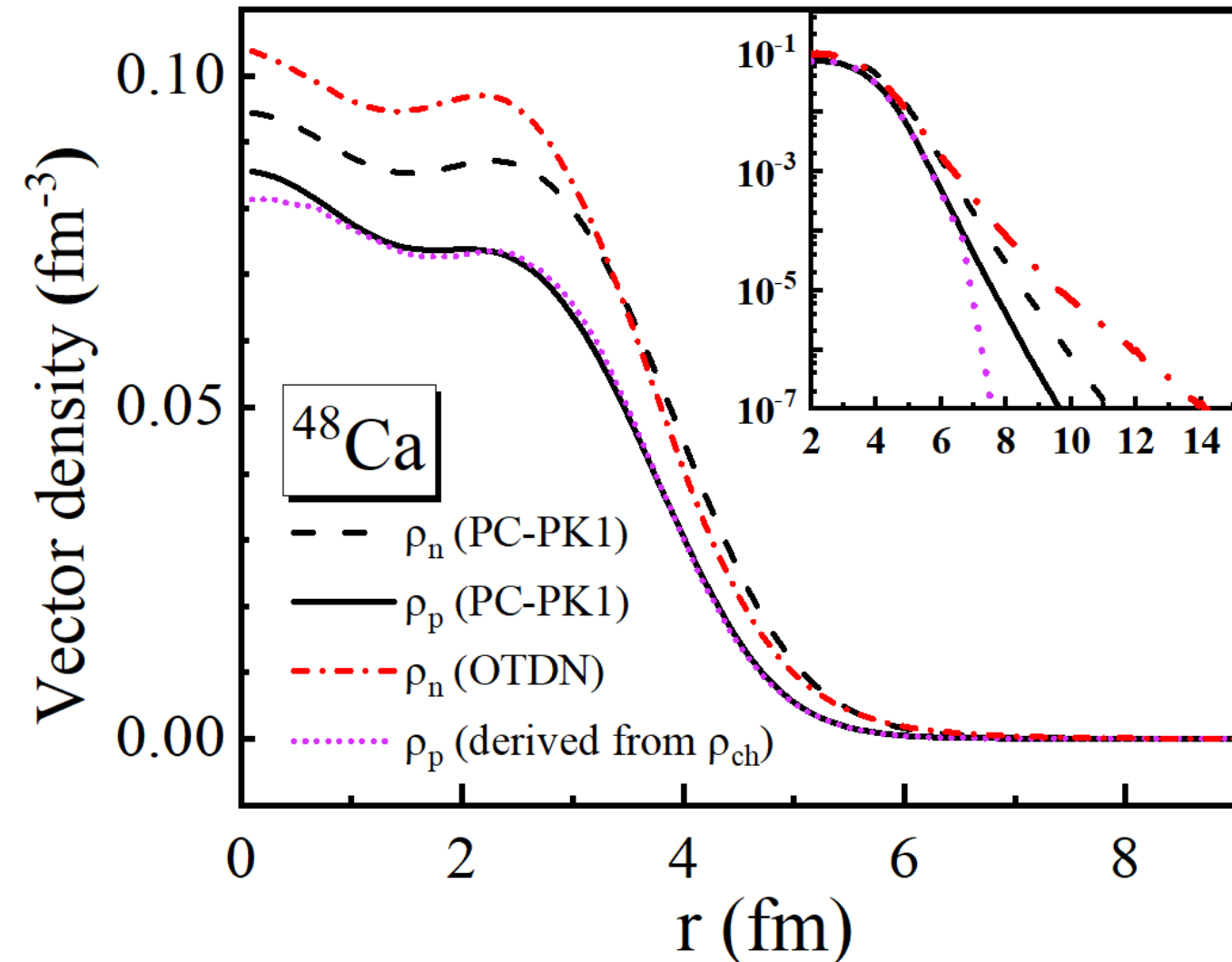
Bayesian Model Averaging (BMA) is a technique that combines models using Bayesian statistical theory. It improves prediction accuracy by averaging multiple models with weights.

- Eliminate the error caused by initializing weights



BMA model weights: $W_k = e^{-\frac{1}{2\sigma} \chi^2} (\sigma = 10)$ 21

Predicted neutron density of ^{48}Ca

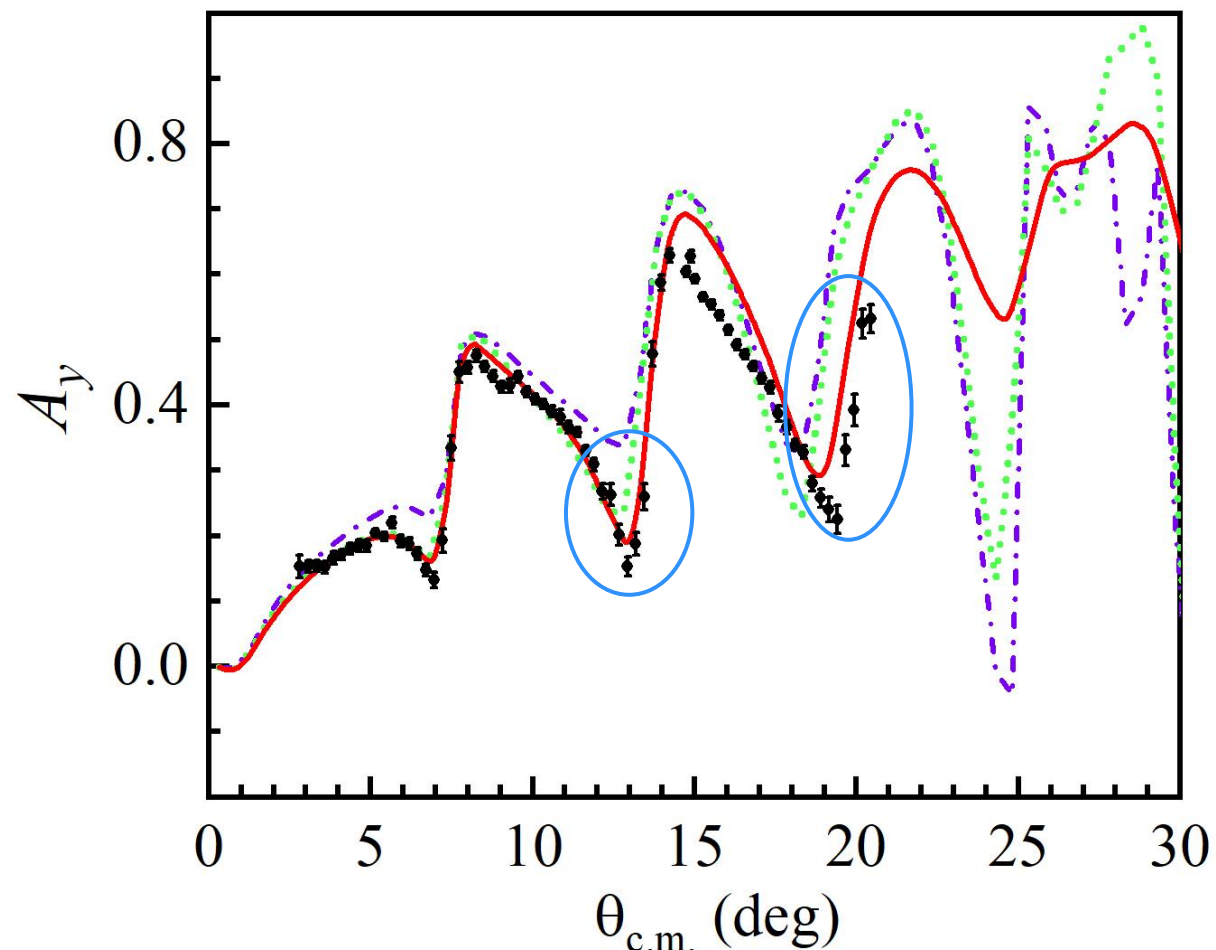
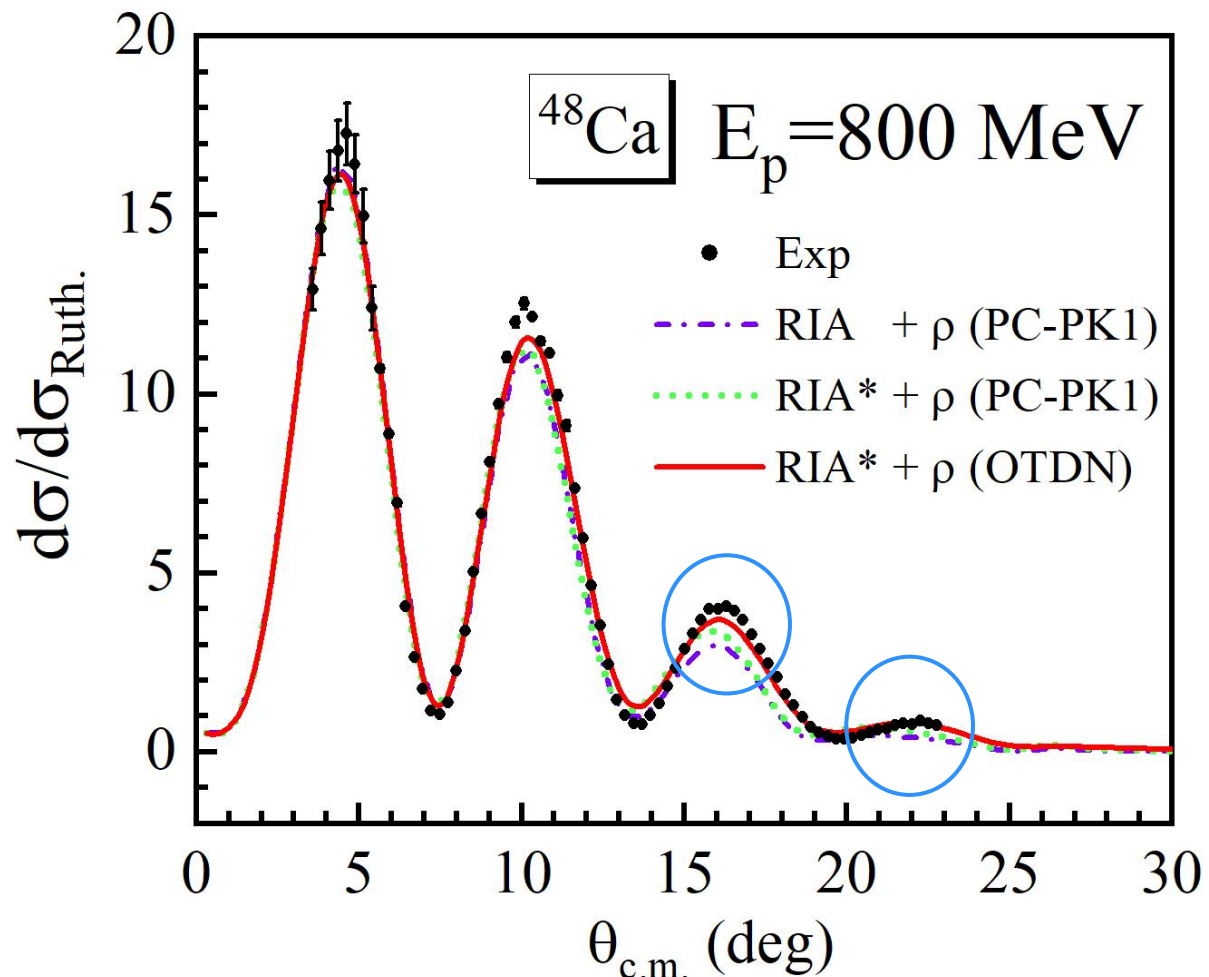


$0 < r < 3$ fm : The predicted neutron density is larger than PC-PK1.

$3 < r < 6$ fm : The predicted neutron density is smaller than PC-PK1.

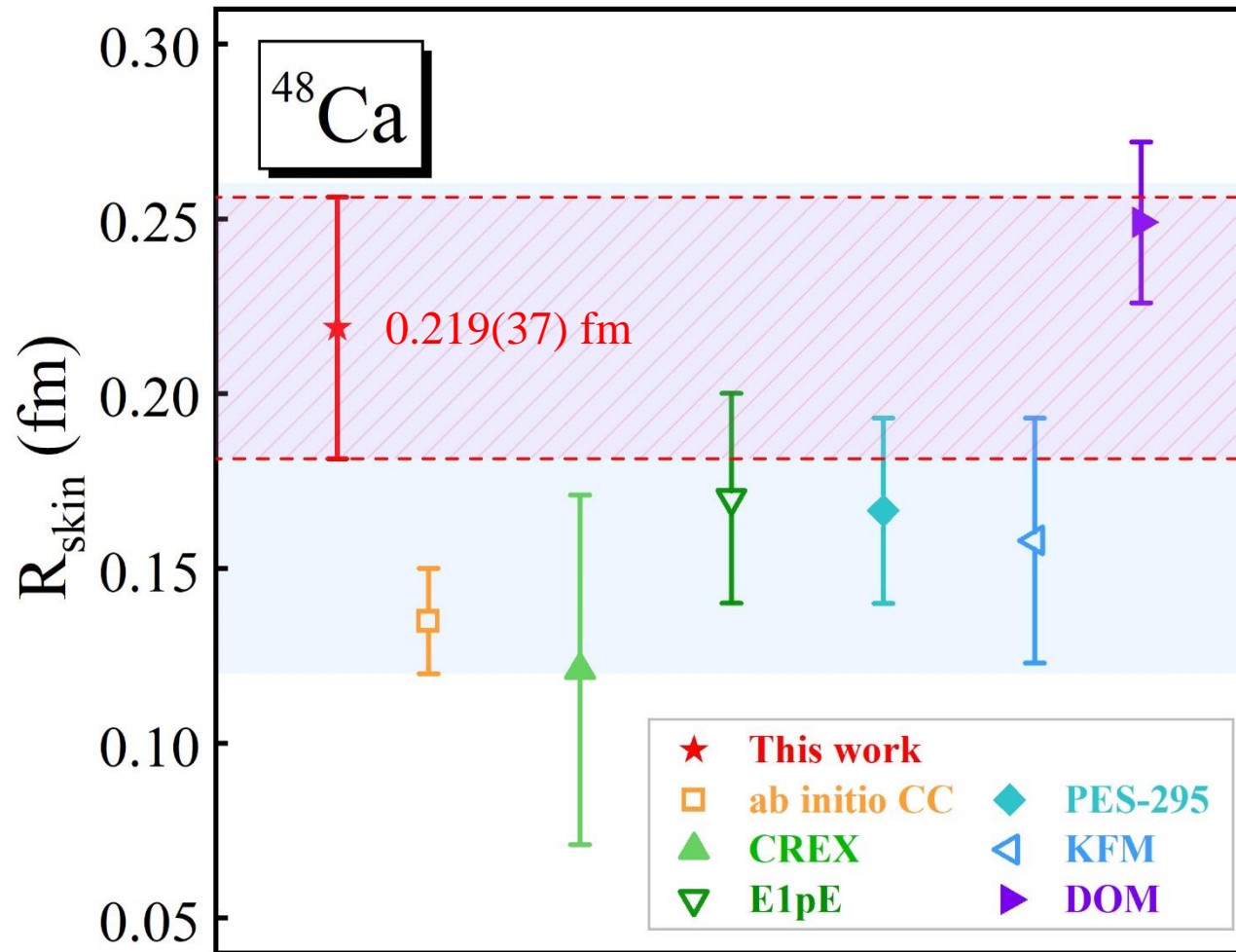
$6 < r < 14$ fm : The predicted neutron density is larger than PC-PK1.

Examine the predicted neutron density of ^{48}Ca



□ Predicted neutron density improves the description at large scattering angles.

Prediction results of neutron skin thickness in ^{48}Ca



□ *ab initio* coupled-cluster (CC)

Hagen, Ekström, Forssén, *et al.*, Nature Physics 12, 186 (2016).

▲ CREX collaboration

Adhikari, *et al.* (CREX Collaboration), PRL 129, 042501 (2022).

▼ E1 polarizability experiment (E1pE)

Birkhan, Miorelli, Bacca, *et al.*, PRL 118, 252501 (2017).

◆ Proton elastic scattering at 295 MeV (PES-295)

Zenihiro, Sakaguchi, Terashima, *et al.*, arXiv (2018)

◁ Kyushu (chiral) g -matrix folding model (KFM)

Tagami, Wakasa, *et al.*, Results in Physics 33, 105155 (2022).

▶ Dispersion optical model (DOM)

Mahzoon, Atkinson, Charity, *et al.*, PRL 119, 222503 (2017).

■ 48 reasonable energy density functionals (EDFs)

Mahzoon, Atkinson, Charity, *et al.*, PRL 119, 222503 (2017).

□ The neutron skin thickness is larger than other studies, except DOM.



Contents



- Introduction
- Back-propagation neural network based on relativistic impulse approximation theory
- Results and discussion
- Summary

- ❑ Considering density-dependent coupling constants in the NN interaction gives the RIA theory with medium effects.
- ❑ A back-propagation neural network (OTDN) based on RIA theory with medium effects is developed
 - ✓ The neutron density distribution of ^{48}Ca is extracted, showing larger values for $r < 3$ fm and $r > 6$ fm compared to PC-PK1, and improving the description of observables at large scattering angles.
 - ✓ The neutron skin thickness is predicted to be $R_{\text{skin}}^{48\text{Ca}} = 0.219(37)$ fm.

DOI: <https://doi.org/10.48550/arXiv.2311.11676>

Appendix 1

Neural network parameters.



Cell-1			
L	Type	D	$g(x)$
—	Input ₁	75	—
1	Linear	128	ReLU
2	Linear	256	ReLU
—	Output ₁	256	—
Cell-2			
L	Type	D	$g(x)$
—	Input ₂	69	—
1	Linear	128	ReLU
2	Linear	256	ReLU
—	Output ₂	256	—
Cell-3			
L	Type	D	$g(x)$
—	Input ₃	160	—
1	Linear	128	ReLU
2	Linear	256	ReLU
—	Output ₃	256	—
Cell-4			
L	Type	D	$g(x)$
—	Output ₁ \uplus Output ₂ \uplus Output ₃	768	—
1	Linear	768	ReLU
2	Linear	1024	ReLU
—	Output ₄	1024	—
Cell-5			
L	Type	D	$g(x)$
—	Output ₄	1024	—
1	Linear	512	ReLU
2	Linear	256	ReLU
3	Linear	160	Sigmoid
—	Output ₅	160	—
Other hyperparameters		Values and Properties	
Numerical Normalization Factor		10	
Loss Function		NPD	
Optimizer		Adam	
Epoch 0-1000		$lr = 1 \times 10^{-2}$	
Epoch 1000-2000		$lr = 1 \times 10^{-3}$	

Real parameters					
Meson	Isospin	Coupling type	m	g^2	Λ
σ	0	Scalar (S)	650	-8.3320	771.6
ω	0	Vector (V)	782	7.0920	803.4
t_0	0	Tensor (T)	1400	-0.6031	1486.0
a_0	0	Axial vector (A)	1200	-0.5023	3488.0
η	0	Pseudoscalar (P)	450	-14.32	450.1
δ	1	Scalar (S)	500	-0.3646	4041.0
ρ	1	Vector (V)	770	0.3485	1149.0
t_1	1	Tensor (T)	450	0.1044	595.6
a_1	1	Axial vector (A)	800	-6.525×10^{-2}	820.0
π	1	Pseudoscalar (P)	138	12.31	557.5
Imaginary parameters					
Meson	Isospin	Coupling type	\bar{m}	\bar{g}^2	$\bar{\Lambda}$
σ	0	Scalar (S)	1300	-4.5500	1553.0
ω	0	Vector (V)	700	2.2100	1479.0
t_0	0	Tensor (T)	550	-0.1078	709.3
a_0	0	Axial vector (A)	750	-0.4360	751.0
η	0	Pseudoscalar (P)	500	7.4180	632.7
δ	1	Scalar (S)	500	0.1295	743.0
ρ	1	Vector (V)	500	-6.6280×10^{-3}	531.5
t_1	1	Tensor (T)	450	-1.1760×10^{-2}	1160.0
a_1	1	Axial vector (A)	850	-0.1116	860.0
π	1	Pseudoscalar (P)	450	2.2470	1246.0

	m^*/m	K	J	L	Ksym	Rskin-208	Rskin-48	Refs.
SIII	0.760	355.370	28.160	9.910	-393.730	0.137	0.125	[2]
SKP	1.000	200.970	30.000	19.680	-266.600	0.144	0.144	[3]
SGII	0.790	214.700	26.830	37.620	-145.920	0.136	0.147	[4]
UNEDF1		219.800	29.000	40.000	-179.400	0.158	0.159	[5]
SkM*	0.790	216.610	30.030	45.780	-155.940	0.170	0.155	[6]
SLy4	0.690	229.900	32.000	45.900	-119.700	0.162	0.152	[7]
SkT3	1.000	235.740	31.500	55.310	-132.050	0.182	0.173	[8]
SGI	0.610	262.000	28.300	63.900	-51.990	0.196	0.180	[4]
Ska	0.610	263.160	32.910	74.620	-78.460	0.214	0.190	[9]
SV-sym34	0.900	234.070	34.000	81.000	-79.080	0.227	0.198	[10]
SK255		254.960	37.400	95.000	-58.300	0.247	0.208	[11]
SkI5	0.580	255.800	36.697	129.300	159.500	0.272	0.214	[12]
12 other groups								[13] J. Friedrich and P.-G. Reinhard, Phys. Rev. C 33, 335 (1986) . [13]